Electronic Supplementary Material (ESI) for Chemical Science

Supporting information

The hidden force opposing ice compression

Chang Q Sun, Xi Zhang, Weitao Zheng
E-mail: *Ecqsun@ntu.edu.sg*

The great seal of truth is simplicity.
- Leonardo da Vinci

1. Extended Ice Rule

As illustrated in Figure 1, the extended Ice Rule can be expressed as follows:

(a) Extended tetrahedron including four identical H bonds connecting the central O^{2-} to the corner O^{2-} . The central tetrahedron is the "two-in two-out" Ice Rule of Pauling.[1]

(b) The"O^{2-} : $H^{+/p}$-O^{2-}"bondrepresents the average of all O---O interactions in most phases unless at extreme conditions [2] in spite of the topological and structural fluctuations [3, 4]. **Coulomb repulsion between the unevenly-bounded nonbonding lone pair ":" and the bonding pair "-"of electrons makes the H-bond flexible and polarizable.** The resultant force of compression, repulsion, and recovery of electron pair dislocations and the incorporative responses of the electron pairs to applied stimuli dictate the relaxation dynamics and hence H_2O anomalies.

(c) In all TIPnQ models, the gas-phase geometry is used for the water molecule, with a bond length of r_{OH} = 0.9572 Å and a bond angle of θ_{HOH} = 104.52°. The TIP4Q model has a positive point charge q_O on the oxygen, a positive point charge q_H on each hydrogen and a negative point charge q_M on a site M located at a distance l_{OM} from the oxygen atom along the bisector of the HOH bond angle. The molecule is electrically neutral thus q_M=-($2q_H$+q_O). q_H, q_O, l_{OM}, σ_{OO} and ε_{OO} areindependent parameters to be determined.σ_{OO} and ε_{OO} are the L-J parameters for O---O interaction.

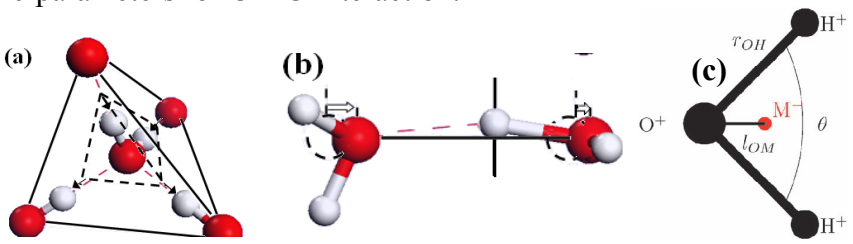

Figure 1Comparison of (a) the extended Ice Rule and (b) the segmentation of the representative H-bondwith (c) the rigid non-polarizable TIP4Q/2005 model for H_2O molecule.[5]

2. The asymmetric relaxation of two segments of H-bond

Table I and Table II show the original data of H-bond length, density and band gap calculated by MD and DFT. Figure 2 shows the deformation electronic density calculated by DFT.

Table I MD derived lengths of the H-bond segments and the resultant length of the O---O of ice.

P(GPa)	O-H (Å)	O:H (Å)	O-O(Å)
1	0.97358	1.76708	2.74066
5	0.97901	1.76247	2.74148
10	0.98527	1.75041	2.73568
15	0.99125	1.72133	2.71258
20	1.00245	1.6919	2.69435
d_0	0.9741	1.7683	2.7415
$\alpha(10^{-4})$	9.510	-3.477	1.717
$\beta(10^{-5})$	2.893	-10.28	-5.835

Table II DFT derived lengths of the hydrogen bond segments, the mass density and the band gap of ice as a function of P.

P(GPa)	□(g/cm^3)	O-H (Å)	O:H (Å)	E_G(eV)
1	1.659	0.966	1.897	4.531
5	1.886	0.972	1.768	4.819
10	2.080	0.978	1.676	5.097
15	2.231	0.984	1.610	5.353
20	2.360	0.990	1.556	5.572
25	2.479	0.996	1.507	5.778
30	2.596	1.005	1.460	5.981
35	2.699	1.014	1.419	6.157
40	2.801	1.026	1.377	6.276
45	2.900	1.041	1.334	6.375
50	2.995	1.061	1.289	6.459
55	3.084	1.090	1.237	6.524
60	3.158	1.144	1.164	6.590

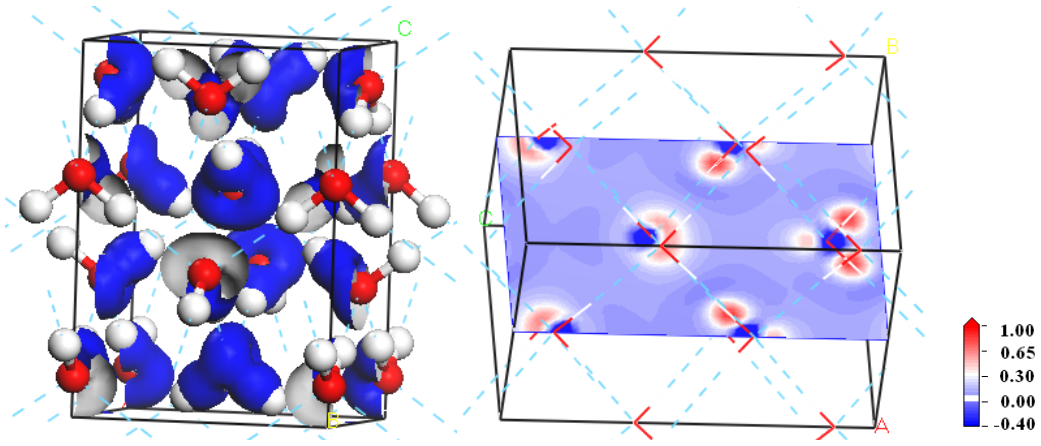

Figure 2(a) DFT-derived deformation electron density of the ice-VIII unit cell with isosurface 0.1electrons/Å^3. Deformation density is the electron density subtracted by the density of the isolated atoms. (b) The positive regions correspond to bonds with gain of electrons and the negative regions (in blue) to electron loss. Electrons transfer from atomic core to the H-O bond and O: H nonbond. **The strong localization of the residual charges evidences the repulsion between the electron pairs.**

3. Stability of DFT Calculations:

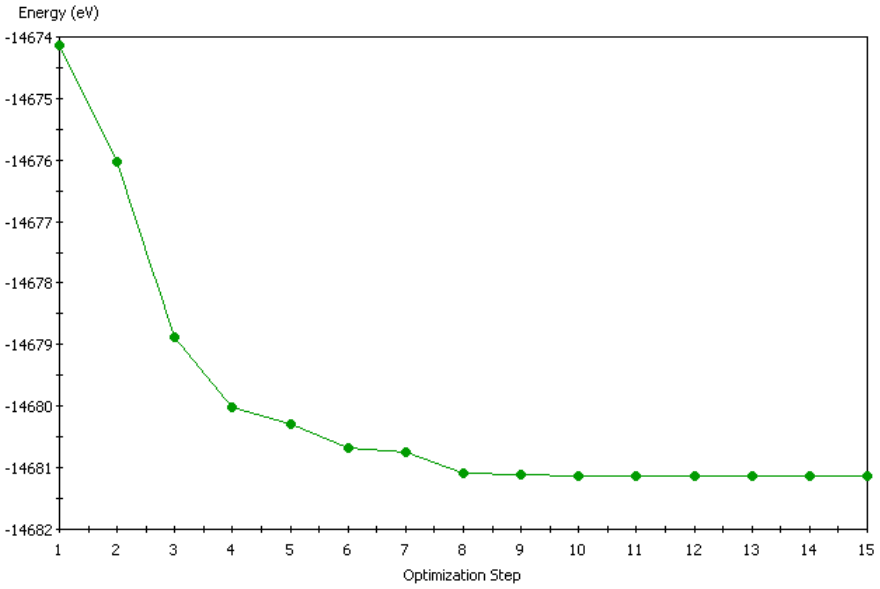

Figure 3 Energy evolvement in the geometry optimization process of iceVIII under 10GPa calculated by DFT.

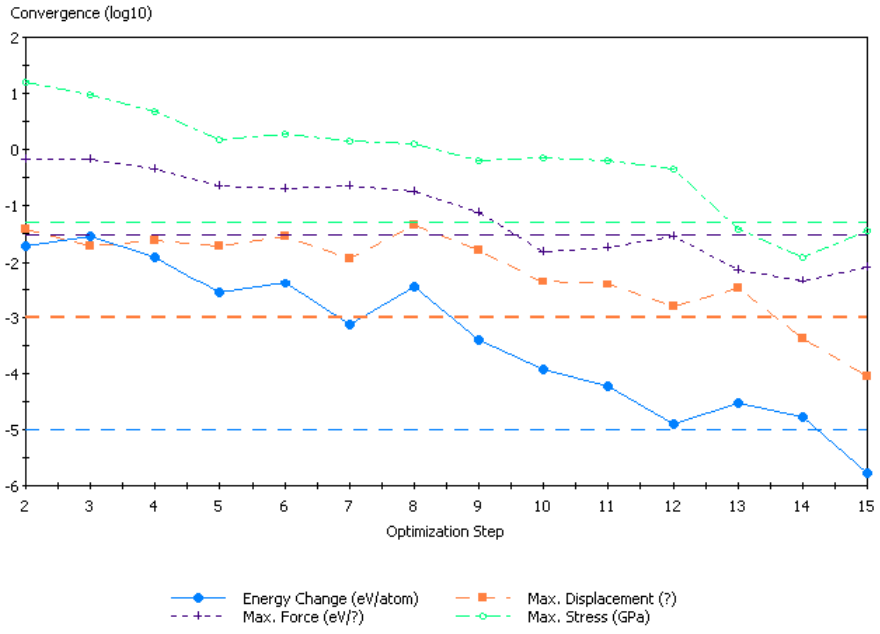

Figure 5 Convergence of energy, force, displacement and stress in the geometry optimization process of iceVIII under 10GPa calculated by DFT.

4. Stability of MD calculation:

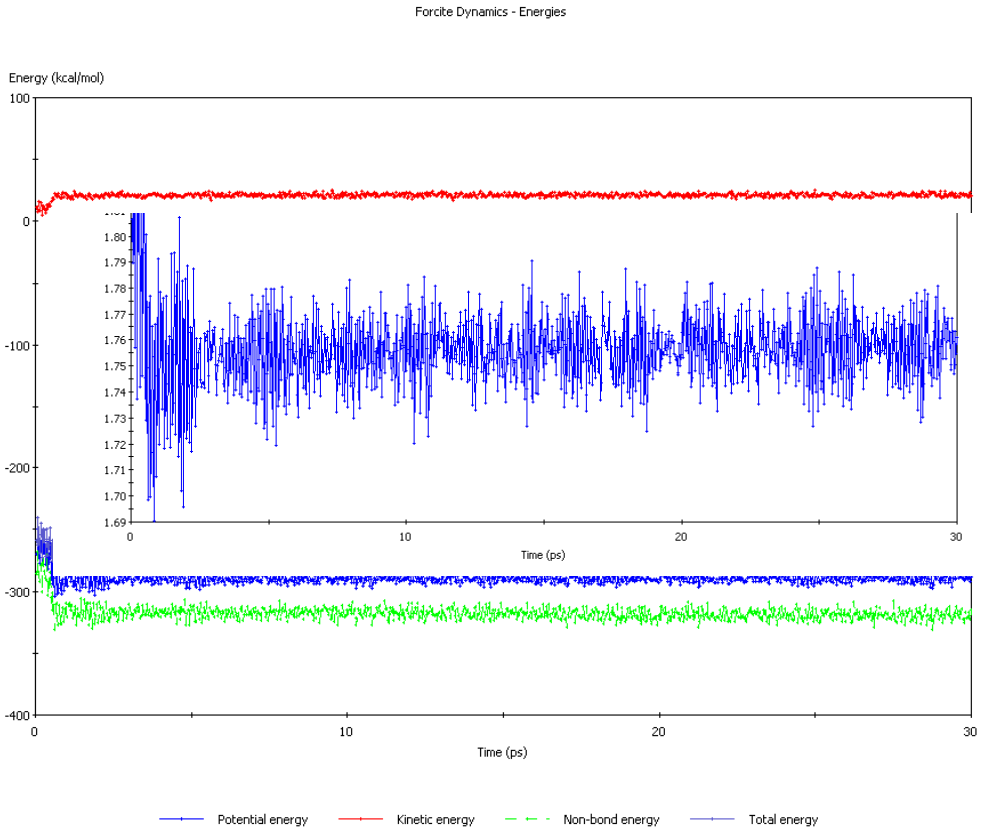

Figure 3 The MD convergences of the potential energy, kinetic energy, non-bond energy and total energy simulation of ice-VIII 2×2 supercell in Isoenthalpic–isobaric ensembleat 5GPa. Inset shows the MD density convergence at 5GPa at 1.755±0.25 g/cm^3.

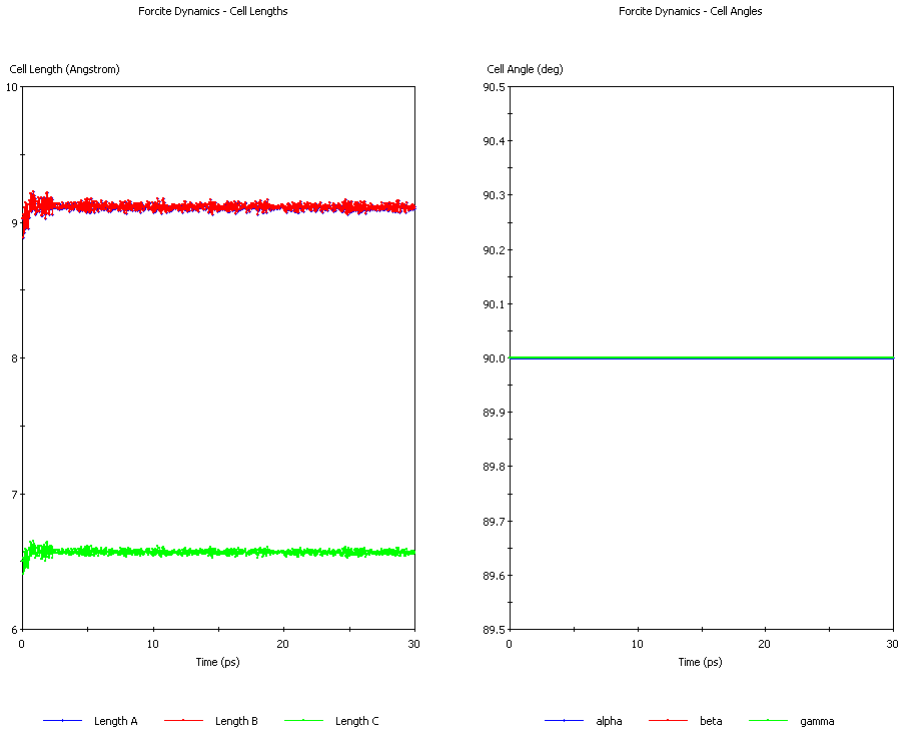

Figure 4 The MD convergences of cell lengths and cell angles at 5GPa.

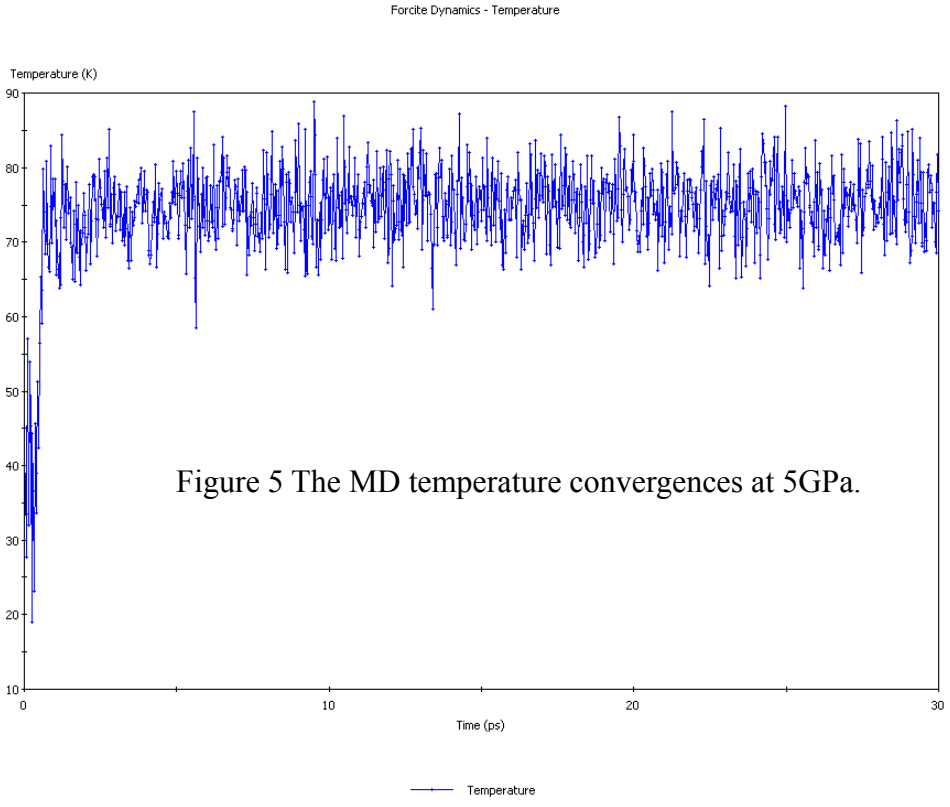

Figure 5 The MD temperature convergences at 5GPa.

5. DFT-derived electronic structure of iceVIII at different P:

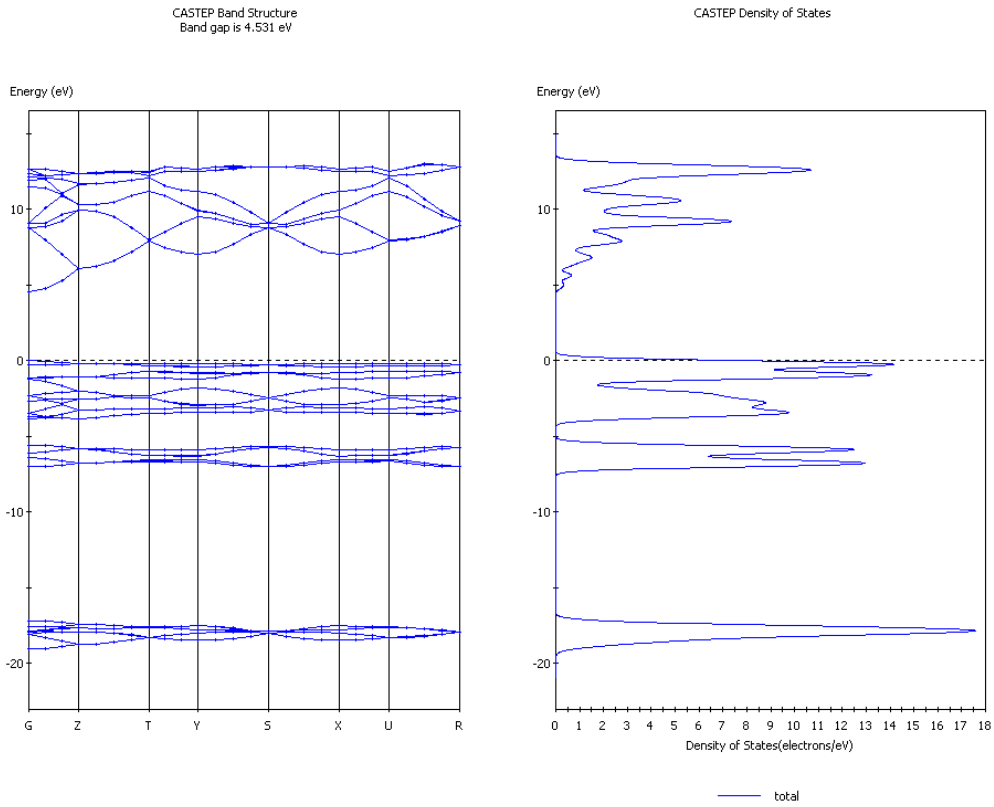

Figure 6DFT-derived energy dispersion (left) and the density of states (DOS, right) of ice-VIII optimized at 1GPa, showing the E_G value and the localized valence DOS.

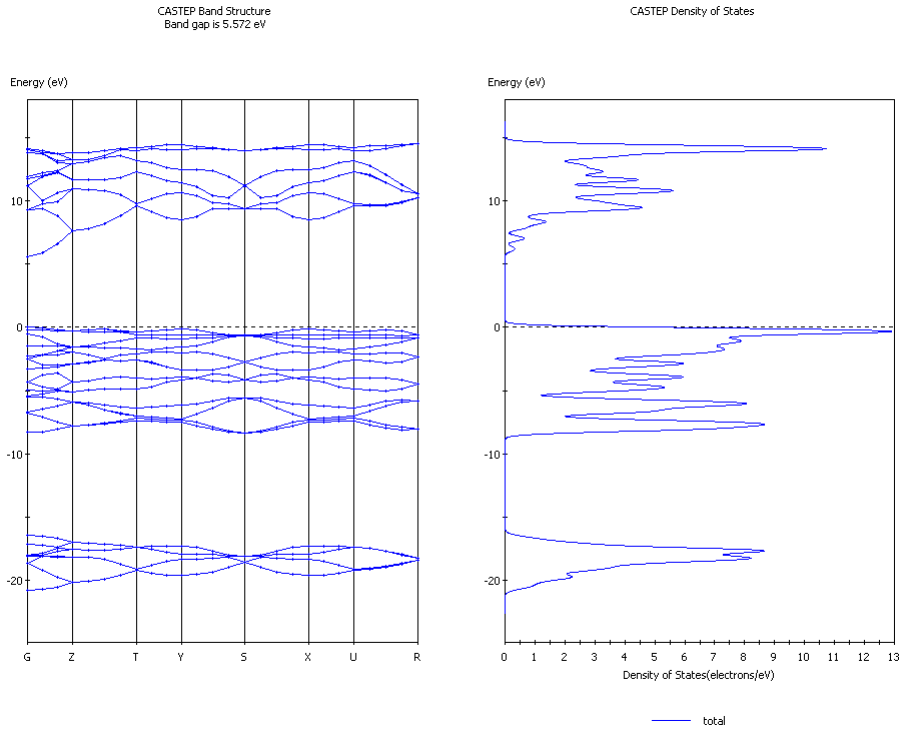

Figure 7 DFT-derived dispersion (left) and DOS (right) of iceVIII at 20GPa, showing the E_G expansion and the deeper shift of the valence DOS.

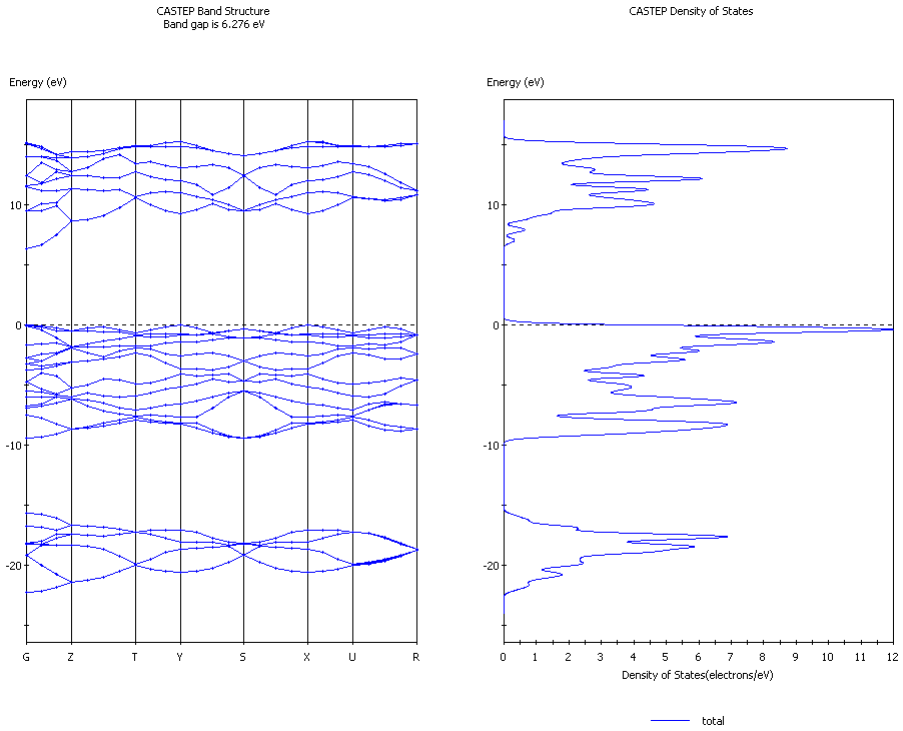

Figure 8 DFT-derived dispersion and DOS of iceVIII at 40GPa.

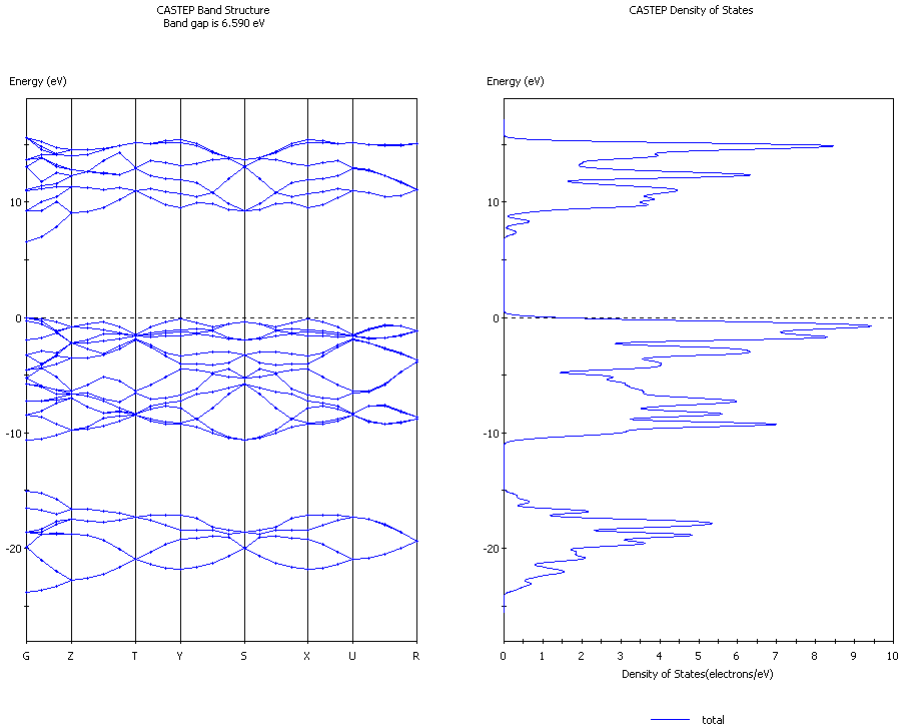

Figure 9 DFT-derived dispersion and DOS of iceVIII at 60GPa. $E_G$increases to 6.590eV.

1. Pauling, L., *The structure and entropy of ice and of other crystals with some randomness of atomic arrangement.* Journal of the American Chemical Society, 1935. **57**: p. 2680-2684.
2. Wang, Y., et al., *High pressure partially ionic phase of water ice.* Nat Commun,

2011. **2**: p. 563.

3. Soper, A.K., J. Teixeira, and T. Head-Gordon, *Is ambient water inhomogeneous on the nanometer-length scale?* Proceedings of the National Academy of Sciences of the United States of America, 2010. **107**(12): p. E44-E44.
4. Huang, C., et al., *The inhomogeneous structure of water at ambient conditions.* Proceedings of the National Academy of Sciences, 2009. **106**(36): p. 15214-15218.
5. Alejandre, J., et al., *A non-polarizable model of water that yields the dielectric constant and the density anomalies of the liquid: TIP4Q.* Physical Chemistry Chemical Physics, 2011. **13**: p. 19728-19740.